

FORMULATION, OPTIMIZATION AND *IN VITRO* CHARACTERIZATION OF ANTIFUNGAL TRANSFEROSOMAL GEL USING BOX-BEHNKEN DESIGN: A CUTTING-EDGE APPROACH TO DRUG DELIVERY

KIRAN RAJKUMAR RAMTIRTHE, PANUGHANTI SUSHMA*, SHAILAJA SHAKAPURAM

Siddhartha Institute of Pharmacy, Narapally, Ghatkesar, Hyderabad, Telangana, India.

Corresponding author:

PANUGHANTI SUSHMA

Assistant Professor

Siddhartha Institute of Pharmacy,

Narapally, Ghatkesar, Hyderabad, Telangana, India.

E-Mail id: panughantisushma_xf@siddhartha.co.in

Mobile No.: +91 81062 51309

ABSTRACT

Background: Transferosomes are ultra-deformable lipid vesicles composed of phospholipids, surfactants, and water, designed to enhance the permeability of drugs through the skin and mucosal barriers. The aim of the investigation is to formulate and evaluate the clotrimazole and miconazole-nitrate-loaded transferosomal gel containing antifungal agents for the treatment of fungal infection.

Method: The transferosomes were developed using thin film hydration approach and optimized by Box-Behnken statistical design with different concentrations of phospholipids and surfactants like soya lecithin, span 80 and tween 80 as independent factors and Entrapment Efficiency (%), Particle Size (nm), Zeta Potential (mV) as dependent variables. The developed MI-CTM transferosomes were then embedded in the carbopol 934 gel basis, which was assessed for drug content, pH, spreadability, viscosity, and *in vitro* release kinetic investigations.

Results: The high EE% ranged from $15.6 \pm 0.66\%$ to $80.25 \pm 1.85\%$ for the synthesized transferosomes, while the particle sizes ranged from 145 ± 0.604 nm to 760 ± 0.684 nm, and the zeta potential ranged from -2.8 to -41.8 mV. Transferosomes surface morphology were assessed using a scanning electron microscope, and it was discovered that the vesicles were spherical with smooth surface. The optimal formulation underwent a 24 h *in vitro* release trial, demonstrating superior drug release of 86.94% and 89.87% CDR with first-order kinetics and Peppas model for miconazole nitrate and clotrimazole, respectively, both of which followed non-Fickian transport mechanism.

Conclusion: As a result, both patient compliance and the frequency of drug application are enhanced by miconazole nitrate and clotrimazole in the form of transferosomal gel.

Key words: Transferosomes, transdermal drug delivery system, antifungal, drug release.

INTRODUCTION

Topical drug delivery systems offer numerous advantages, including localized action, which ensures direct delivery to the target site while minimizing systemic side effects and toxicity. They are non-invasive, bypassing the need for injections and avoiding hepatic first-pass metabolism, thus improving bioavailability. These systems provide controlled or sustained drug release, reducing dosing frequency and enhancing patient compliance. Their ease of application makes them suitable for self-administration, particularly in paediatric and geriatric patients [1-3]. Additionally, they offer flexibility in formulation, accommodating a wide range of drugs, and avoid gastrointestinal issues associated with oral medications. Advanced systems like transferosomes further enhance drug penetration into deeper skin layers, improving therapeutic efficacy and making topical delivery a versatile and patient-friendly option. The development of topical drug delivery systems aligns with the growing demand for safe and patient-friendly therapeutic options. In addition to localized treatments, certain formulations have been optimized for transdermal drug delivery, allowing systemic absorption through the skin. This versatility makes topical drug delivery systems a vital component of modern pharmaceutical research and development [4].

Transferosomes are ultra-deformable lipid vesicles composed of phospholipids which form the bilayer structure providing a lipid environment for drug encapsulation, edge activators like surfactants tween 80 and span 80 destabilize the bilayer enhance deformability, making them more elastic and penetration through skin mucosal barriers and water for encapsulating the hydrophilic drugs within the core of the vesicles [5]. Unlike conventional liposomes, transferosomes possess exceptional flexibility, enabling them to traverse narrow intercellular gaps within the skin's stratum corneum. Niosomes lack the deformable nature, making them

less effective for deep skin delivery. Ethosomes are alcohol-based systems, which may cause irritation with long-term use. These features make them particularly suitable for topical drug delivery, offering superior efficacy, better patient compliance, and versatile application compared to other vesicular systems. This unique characteristic makes transferosomes highly effective in delivering both hydrophilic and lipophilic drugs to the deeper layers of the skin and even into systemic circulation when required. They act as a promising carrier system for drugs with limited solubility and permeability [6].

Gels are semi-solid systems composed of a three-dimensional network of polymers that can incorporate both hydrophilic and lipophilic drugs. Their high-water content provides a cooling and soothing effect, making them ideal for topical applications [7]. Gels also offer advantages such as ease of application, uniform drug distribution, and the ability to control drug release over extended periods [8]. When combined with transferosomes, gels serve as a matrix for stabilizing the vesicles, enhancing patient compliance, and allowing sustained release of the drug at the target site [9]. This synergy between transferosomes and gel systems is particularly beneficial for drugs like Miconazole Nitrate and Clotrimazole, which require efficient delivery to deeper skin layers for antifungal action.

Miconazole Nitrate and Clotrimazole are broad-spectrum antifungal agents belonging to the imidazole class. They act by inhibiting the synthesis of ergosterol, an essential component of fungal cell membranes, leading to cell membrane disruption and eventual fungal cell death. However, these drugs face challenges such as Low aqueous solubility (BCS Class II) results in poor absorption and bioavailability. Because of high lipophilicity (Log P =5-6) makes them ideal candidates for lipid-based delivery systems like transferosomes. Both drugs are typically formulated for topical or localized applications, as their systemic absorption is minimal, but their high permeability and lipophilic nature make them effective in penetrating biological membranes for targeted antifungal action. By formulating these drugs into transferosomal gels, it is possible to overcome these challenges. Transferosomes enhance their solubility and permeability, while the gel matrix ensures sustained release and localized delivery, reducing dosing frequency and side effects [10].

The primary aim of this research is to develop and evaluate transferosomal gels containing Miconazole Nitrate (MI) and Clotrimazole (CTM) using the Box-Behnken Design. The study focuses on optimizing formulation parameters to achieve enhanced drug penetration, improved antifungal efficacy, and patient compliance. Thus, transferosomes, a type of ultra-deformable vesicular carrier, have revolutionized topical drug delivery by enabling deeper penetration into the skin. When integrated into a gel matrix, transferosomes can further enhance the therapeutic efficacy of drugs by providing sustained release and ease of application [11]. Such advancements have emerged as innovative solutions for improving the bioavailability and therapeutic efficacy of poorly soluble drugs antifungal agents like Miconazole Nitrate and Clotrimazole.

MATERIALS AND METHODS

Materials

Miconazole nitrate and clotrimazole were the gift samples from Yarrow Chem. products, Mumbai, India. Tween 80, and Span 80 were purchased from HI media laboratories Pvt. Ltd. Hyderabad. Soya Lecithin and Carbopol 940P were procured from S.D. Fine Chem. Ltd, Mumbai, India. Chloroform was obtained from Yarrow Chem. products, Mumbai, India. Methanol and ethanol are purchased from Techno Scientific Products, Bangalore India.

Methods

Preformulation Studies

Melting point determination: The capillary tube method was used to find Miconazole Nitrate and Clotrimazole melt point using the Thiele's tube apparatus. One end of the capillary was sealed off with a flame. The open end of the capillary tube was filled with a small lump of powder, and the tube was gently tapped to allow the powder collect settle. The process was repeated many times. The capillary tube was then put inside the melting point instrument. The temperature at which medicines dissolve was noticed [11].

Solubility studies: Miconazole nitrate and Clotrimazole solubilities in distilled water, ethanol, methanol, and 6.8 pH PBS were assessed using the shake flask technique. To a flask that already contained 10 ml of each solvent, extra medication was added. Following that, the mixtures were heated to 37 °C for two hours while being swirled in a magnetic stirrer at 100 rpm. They were then filtered, diluted, and evaluated spectrophotometrically with a UV spectrophotometer at 232 nm and 263 nm for miconazole nitrate and clotrimazole, respectively, in comparison to an untreated blank [12].

Drug excipient compatibility study using FT-IR: On a pure drug sample, the chemical was recognized using infrared spectroscopy. Infrared spectroscopy was carried out using a Thermo Nicolet FTIR, and the spectrum between 4000 and 400 cm^{-1} was obtained [13]. KBr (200–400 mg) was dissolved in a sample (drug and drug-excipient mixture, 1:1 ratio) and then compacted into discs using a hydraulic press at a pressure of 5 tonnes for 5 min. The spectra were collected using an average of three scans at a resolution of 2 cm^{-1} . The interaction between the excipients and the medication was investigated using IR spectral examinations, which looked for any changes in drug peak locations in the spectrum of a physical mixture of pharmaceuticals.

Optimization of formulations by design of experiment [11]

The formulation and optimization of transferosomes containing miconazole nitrate and clotrimazole drugs were carried out using the Box-Behnken statistical design, a robust response surface methodology that facilitates the systematic evaluation of formulation variables. Independent factors included varying concentrations of phospholipids (soya lecithin) and surfactants (Span 80 and Tween 80), which are critical components influencing the vesicular characteristics. The dependent variables Entrapment Efficiency (%), Particle Size (nm), and Zeta Potential (mV) were selected as key parameters to evaluate the performance and stability of the transferosomal formulations. This design enabled the identification of optimal formulation conditions while minimizing experimental runs and understanding factor interactions.

Preparation of transferosomes: The transferosomes were made using the conventional thin film hydration method using rotary flash evaporator [14]. Specifically, a clean, dry, round-bottom flask was filled with the medication, phospholipid, and surfactant. The lipid combination was subsequently dissolved in a solution of 2:1 volume ratio chloroform to methanol. Rotary evaporation was used to evaporate the organic solvent at 60°C under reduced pressure. Overnight, final solvent remnants were vacuumed out. Rotating at 60 revolutions per minute for one hour at room temperature, the deposited lipid film was hydrated with 6.8 pH buffer (above the lipid transition effects). Large multilamellar vesicles (LMLV) were produced after the resulting vesicles were enlarged for two hours at room temperature. LMLVs were ultrasonically processed for 20 min at 4 °C to create smaller vesicles.

Formulation of transferosomal gel: By employing the rotary flask evaporation method and 1% weight/weight of carbopol 940 P as the gel base, miconazole nitrate and clotrimazole-loaded transferosomal gel was created. The transferosomal solution mentioned above was then mixed continuously with carbopol, methyl paraben, and propyl paraben, which were used as preservatives in a 10:1 ratio and dissolved in propylene glycol, until a homogenous gel was produced [15].

Evaluation of Transferosomes [16,17]

Determination of entrapment efficiency (%EE)

Total transferosomal suspensions underwent a 30-minute ultracentrifugation at 20,000 rpm and 10 °C. Following centrifugation, 50 ml of 6.8 pH buffer were added to dilute 1 ml of supernatant, and the absorbance of miconazole nitrate and clotrimazole was then measured using a UV-Vis spectrophotometer at 232 nm and 263 nm, respectively. The following formula was used to compute the drug entrapment efficiency:

$$EE (\%) = \frac{\text{Total amount of drug} - \text{Untrapped drug}}{\text{Total amount of drug}} \times 100$$

Photo-Microscopic Analysis and Scanning Electron Microscope [18]

The vesicles were examined using an optical microscope, and images of them at a 10x magnification were taken with a camera attachment. To ascertain the morphology of the optimized formula, SEM examination was employed. One drop of an optimized transferosomal suspension was applied to a collodion-coated copper grid, and it was kept there for around two minutes to allow the transferosomes to adhere to the collodion and dry. Then, a drop of uranyl acetate solution was added, and a grid was allowed to sit for a minute. A SEM analysis was carried out after the material had dried.

Determination of Particle Size and Zeta Potential [19]

To determine particle size, zeta potential, and polydispersity index for all manufactured Transferosomes (TFS), the dynamic light scattering (DLS) method was applied at 25 °C with a Malvern Zetasizer (Malvern, UK). Before measurements were taken, the TFS-loaded transferosomal colloidal dispersion was diluted with purified water (phosphate buffer).

Characterization of Transferosomal Gel containing antifungal drugs [18,20]

Homogeneity

Determining the homogeneity of semisolid dose forms that are applied topically to the skin is crucial for patient compliance. A little amount of MI-CTM loaded transferosomal gel was compressed between the thumb and index finger to accomplish this. The homogeneity of the consistency was assessed.

Determination of pH

The pH of transferosomal gel formulation was determined by using calibrated pH meter. The readings were taken for average of 3 samples.

Spreadability

By pressing 1 gramme of gel between two clear, spherical glass slides, the spreadability of each batch of transferosomal gel was evaluated. They were allowed to spread out for a maximum of five minutes. To determine the spreadability, the diameter of produced circle was measured.

Determination of drug content

To a beaker of precisely weighed topical transferosomal gel equivalent to 100 mg, 20ml of phosphate buffer was added. Whatman filter paper no. 1 was used to filter this mixture after it had been fully mixed. Then, using phosphate buffer, 1.0 mL of the filtered solution was added to a volumetric flask with a 10 mL capacity. This solution was examined using a UV-Spectroscope at maximum wavelength of 232 nm and 263 nm for miconazole nitrate and clotrimazole, respectively, and the following formula can be used to compute the percentage of drug content.

$$\% \text{ Drug content} = \frac{\text{Practical drug content}}{\text{Theoretical drug content}} \times 100$$

Viscosity and rheological studies

The viscosity of MI-CTM loaded transferosomal gels was measured by a Brookfield viscometer using spindle number 4 rotated at a speed of 5 to 25 rpm at 25 °C [21].

In vitro drug release studies

Franz diffusion cells and a dialysis membrane were used for *in vitro* diffusion research [22]. 20 ml of 6.8 pH PBS and 1 gramme of transferosomal gel loaded with MI-CTM were placed in the donor and recipient compartments, respectively. At predetermined intervals, 2 ml aliquots of samples were taken from the sampling port. A similar volume of brand-new dissolving medium was used in place of the removed samples. The experiment was carried out in triplicate, and the means and standard deviations were measured. Using a UV spectrophotometer, the samples were examined for miconazole nitrate and clotrimazole, respectively, at 232 nm and 263 nm. A 24 h release study was conducted. Time and the total amount of medication released were plotted.

Short term Stability Studies

Stability of a pharmaceutical product may be defined as the capability of a particular formulation, in a specific container, to remain within its physical, chemical, therapeutic and toxicological specifications throughout its shelf life [23].

ICH specifies the length of study and storage conditions.

Long Term testing: 25°C ± 2°C / 60% RH ± 5% for 12 months

Accelerated Testing: 40°C ± 2°C / 75% RH ± 5% for 6 months

Method: Ideal formulations of MI-CTM loaded transferosomal gel were subjected to accelerated stability testing as per ICH guidelines for short term and stored in screw capped, amber coloured small glass bottles. Analyses of the samples were characterized for drug content, pH and *in-vitro* drug release for the period of 3 months [24].

RESULTS AND DISCUSSION

Miconazole nitrate and Clotrimazole loaded transferosomes were prepared using thin film hydration method by applying design of expert (DOE). The total of twenty batches of transferosomes were prepared, where the concentration of drugs was kept constant and the ratio of lipid: surfactant was varied. Transferosomes were then assessed for their morphology, particle size, zeta potential and entrapment efficiency and on the basis of these factors selection of optimized formulation has been done for the formulation of transferosomal gel. Then the transferosomes were dispersed in carbopol 940P to form transferosomal gel.

Preformulation Studies

Solubility profile of Miconazole Nitrate and Clotrimazole

Determining a drug's solubility and stability in various solvents is one of the key objectives of the pre-formulation process. The shake-flask method was used to determine miconazole nitrate and clotrimazole solubility. Table 1 and Table 2 shows the solubility of miconazole nitrate and clotrimazole in various solvents respectively.

Table 1: Solubility Profile of Miconazole Nitrate in different solvents

Solvents	Solubility ± SD (mg/ml)	Parts of solvents required for one parts of solute	Description term
Distilled Water	<0.001	More than 10000	Practically insoluble

pH 6.8PBS	2.18	100-1000	Slightly Soluble
Ethanol	45.43	1-10	Freely Soluble
Methanol	45.43	1-10	Freely Soluble
Chloroform	8.43	From 10-30	Sparingly Soluble

Table 2: Solubility profile of Clotrimazole in different solvents

Solvent	Solubility \pm SD (mg/ml)	Parts of solvent required to one part of solute	Description term
Distilled water	<0.001	More than 10000	Practically insoluble
pH 6.8 PBS	2.18	From 100-1000	Sparingly soluble
Ethanol	8.43	1-10	Freely Soluble
Methanol	45.43	1-10	Freely Soluble
Chloroform	7.46	From 10-30	Slightly Soluble

Melting Point

Melting point was determined by the capillary tube method for both the drugs by taking average of three trials. The melting point for Miconazole Nitrate and Clotrimazole drug was found to be 184 and 147 °C respectively

Table 3: Melting point of Miconazole nitrate

Trial No.	Melting point (°C)	Average of Melting point (°C)
1	183	184
2	185	
3	184	

Table 4: Melting Point of Clotrimazole

Trial No.	Melting point (°C)	Average of Melting point (°C)
1	146	147
2	148	
3	147	

Drug excipient compatibility studies by FTIR

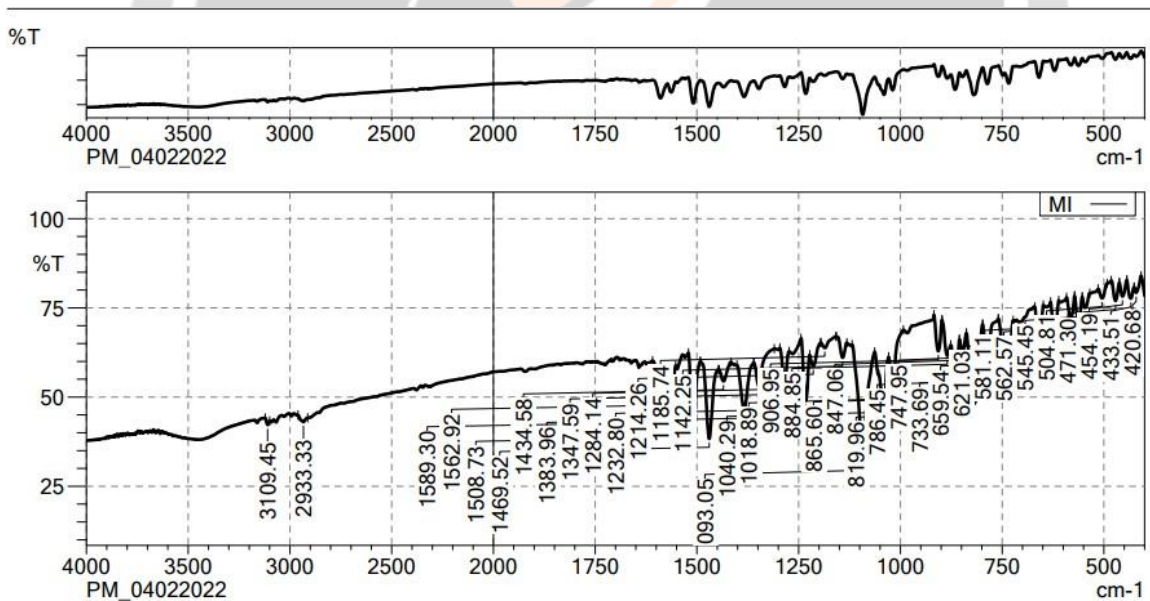
The FTIR spectrum analysis of Miconazole Nitrate (MI) and Clotrimazole (CTM) reveals the presence of key functional groups corresponding to their characteristic absorption peaks. The aliphatic C-H stretching vibration was observed in the range of 2933.33 cm^{-1} for MI and 2925.49 cm^{-1} for CTM. The aromatic C=C stretching appeared between 1469.52–1589.30 cm^{-1} for MI and 1452.41–1565.78 cm^{-1} for CTM, within the standard range of 1615–1450 cm^{-1} . The Ar-O-CH₃ functional group exhibited peaks between 1040.29–1232.80 cm^{-1} for MI. The carbonyl group (C=O) showed a distinct absorption at 1683.4 cm^{-1} for MI, fitting the 25421

typical range of 1800–1600 cm^{-1} . Additionally, the combined $\text{C}\equiv\text{C}$ and $\text{C}=\text{N}$ stretches were observed between 2933.33–3109.45 cm^{-1} for MI and 2925–3166.497 cm^{-1} for CTM, overlapping the specified range of 3300–2500 cm^{-1} . The C-Cl stretch was identified between 733.69–786.45 cm^{-1} for MI and 708.02–765.06 cm^{-1} for CTM. This analysis confirms the structural integrity and functional group characteristics of Miconazole Nitrate and Clotrimazole as per their IR spectral data.

The FTIR spectrum analysis of various physical mixture of Miconazole Nitrate (MI), Clotrimazole (CTM), and excipients such as Soya Lecithin (SL), Span-80 (S80), and Tween-80 (T80), as well as optimized formulation, reveals characteristic absorption peaks that confirm the presence of key functional groups in each formulation. For the aliphatic C-H stretching vibrations, peaks were observed in the range of 2854.19–2925.49 cm^{-1} for MI+SL, CTM+SL, and MI+CTM+SL combinations. The aromatic C=C stretching was observed within the range of 1468.81–1590.02 cm^{-1} across most combinations, with minor variations such as 1547.95 cm^{-1} in MI+CTM+SL and 1455.97 cm^{-1} in MI+CTM+S80. The optimized formula exhibited peaks in the range of 1453.12–1590.02 cm^{-1} . The Aromatic-O- CH_3 group displayed peaks between 1092.34–1232.80 cm^{-1} for MI+SL, CTM+SL, and MI+CTM+SL. A prominent carbonyl group (C=O) stretch was observed at 1741.18 cm^{-1} for MI+SL, CTM+SL, and MI+CTM+SL, and the optimized formulation showed a peak at 1721.21 cm^{-1} . The C-Cl stretching vibrations were evident within 732.98–786.45 cm^{-1} for MI+SL, with slight variations for other combinations, such as 748.66–795.01 cm^{-1} for MI+CTM+S80 and 751.52 cm^{-1} for optimized formulation.

These findings confirm the presence of functional groups associated with MI and CTM across various formulations. Based on the FTIR data, there are no significant shifts or disappearance of characteristic peaks for Miconazole Nitrate (MI), Clotrimazole (CTM), and the excipients (Soya Lecithin, Span-80, and Tween-80) in the various combinations. All functional group peaks, including C-H, C=C, C=O, Ar-O- CH_3 , and C-Cl, remain intact across formulations. This indicates no chemical incompatibility between the drugs and excipients used.

Figure 1: Infrared Spectrum of Miconazole Nitrate



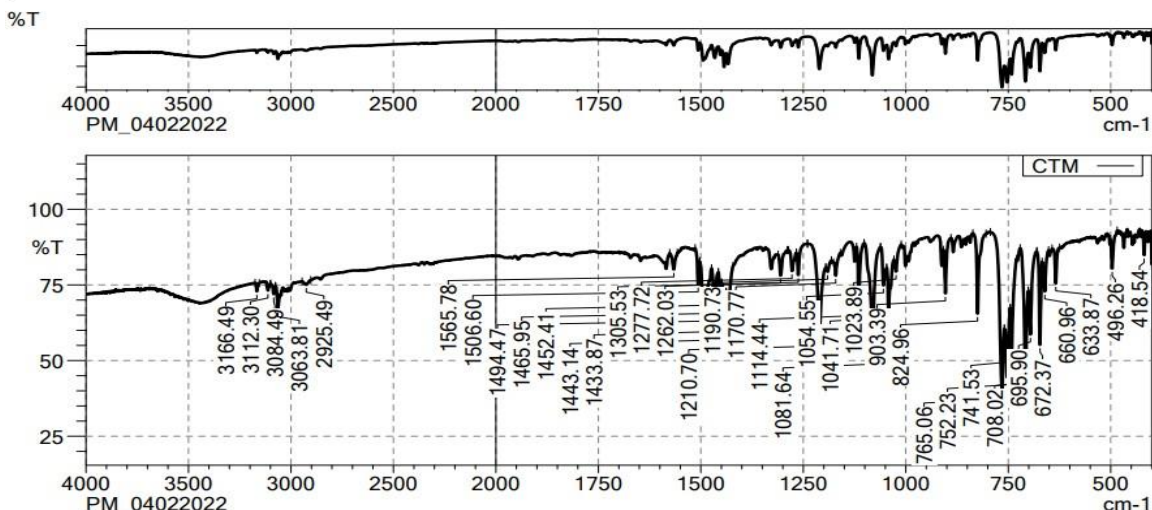


Figure 2: Infrared Spectrum of Clotrimazole

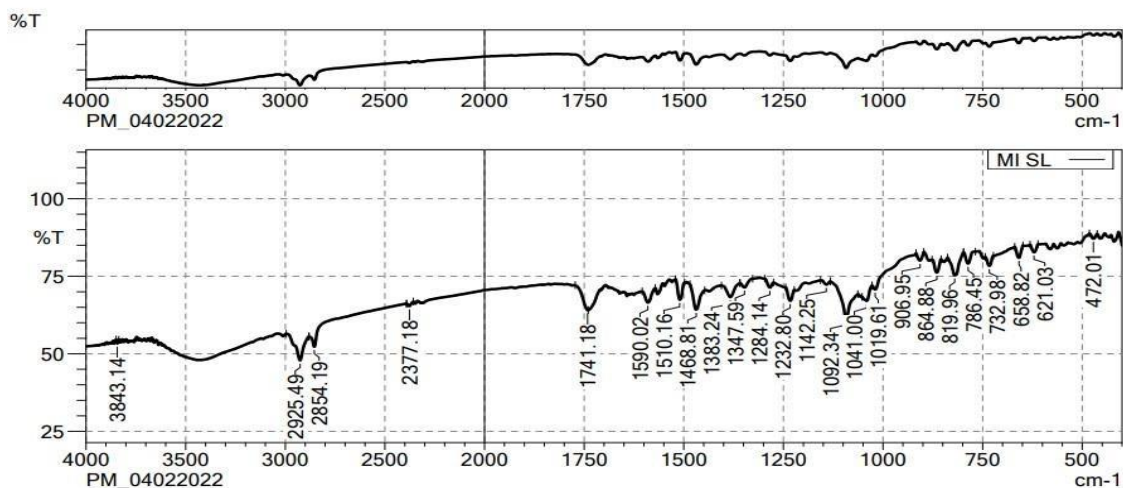


Figure 3: Infrared Spectrum of Miconazole Nitrate and Soya Lecithin

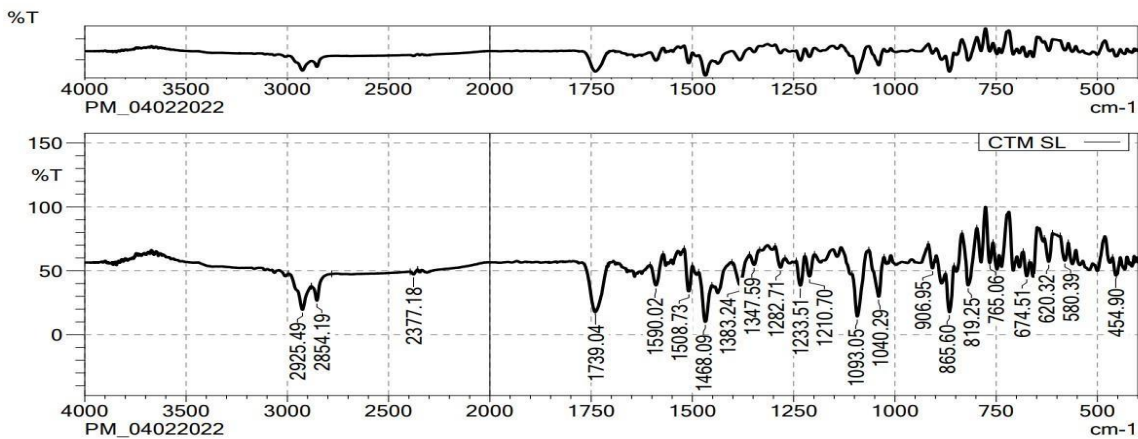


Figure 4: Infrared Spectrum of Clotrimazole and Soya Lecithin

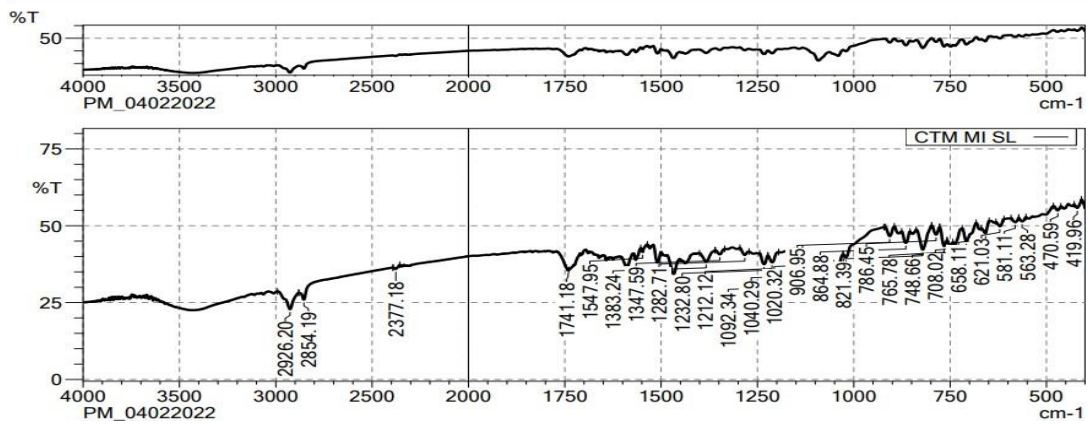


Figure 5: Infrared Spectrum of physical mixture of Miconazole Nitrate, Clotrimazole and Soya Lecithin(SL)

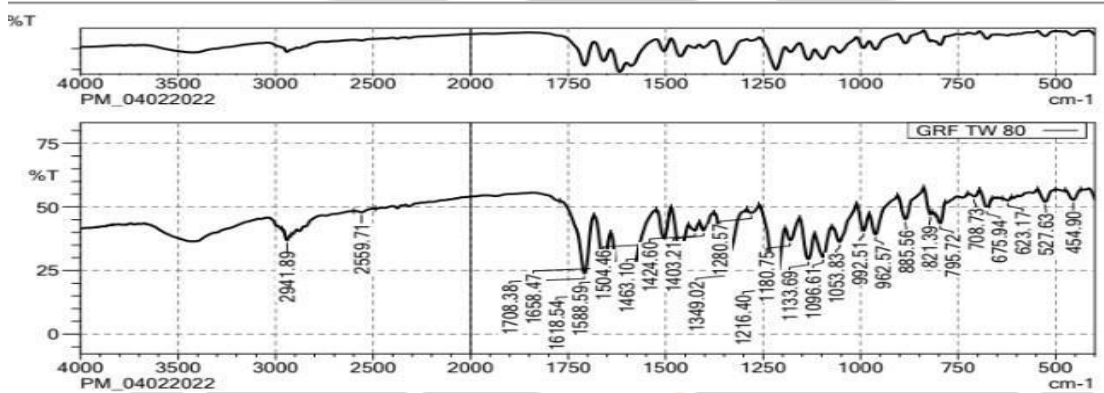


Figure 6: Infrared Spectrum of physical mixture of Miconazole Nitrate, Clotrimazole and Tween-80

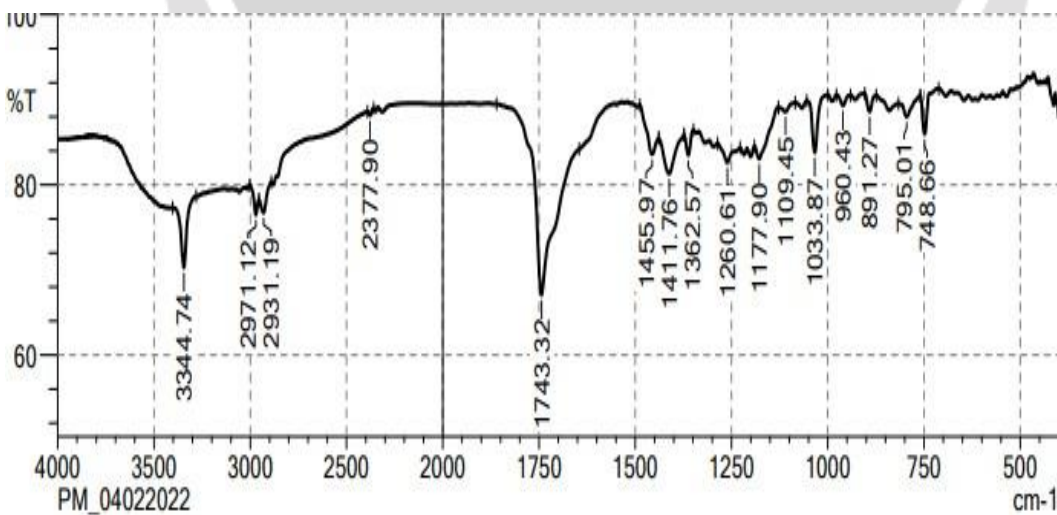


Figure 7: Infrared Spectrum of physical mixture of Miconazole Nitrate, Clotrimazole and span 80

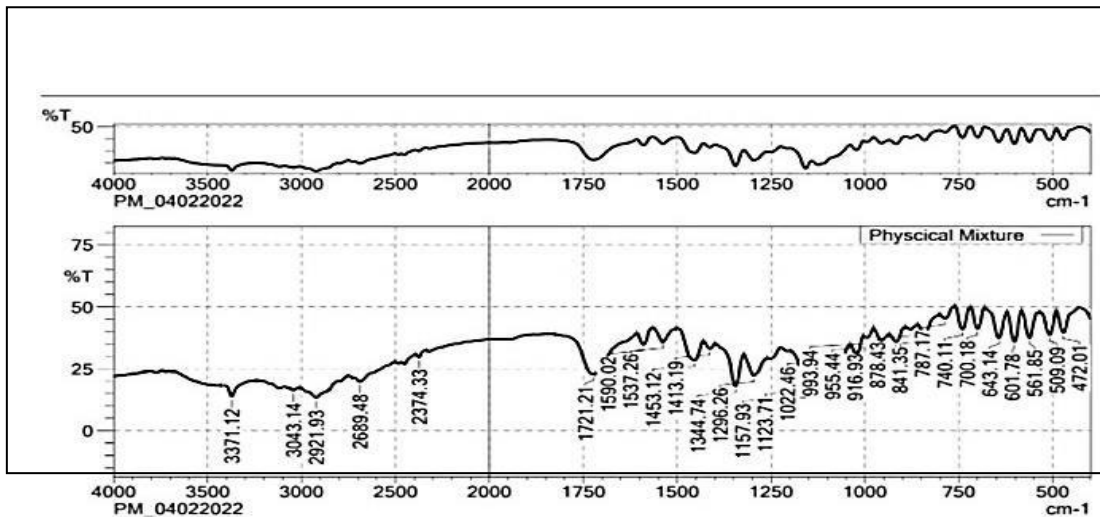


Figure 8: Infrared Spectrum of optimized formulation

Preparation of Transferosomes containing Miconazole Nitrate and Clotrimazole

The maximum entrapment efficiency (EE%), minimum particle size, and optimum zeta potential were determined by examining the effects of a few selected factors and their interactions using Box-Behnken Design. Table 5 presents the projected results of all 20 experimental trials along with the observed responses. The % entrapment efficiency of experimental formulations was the amount of drug entrapped, was ranged between 15.6% to 80.25% and particle size was identified in the range of between 145 to 724.3nm and zeta potential ranges between -2.8 to -41.8mV. To examine all of the experiment findings for the individual responses, the quadratic model and ANOVA were employed [24-26].

Every response was assigned to the quadratic model based on the fit summary and the sequential sum of squares (Type-I). R², p-value, and F-value analyses were done in order to choose a model. Furthermore, the quadratic model has the highest degree of statistical significance in terms of polynomial order, with a p-value of 0.0001.

Table 5: Optimization by Experimental Design: Effect of various Levels of independent factors like Soya Lecithin, Span-80, and Tween-80 on dependent variables

Std	Run	Factor 1	Factor 2	Factor 3	Response 1	Response 2	Response 3
		A:Soyalecithin	B:Span-80	C:Tween-80	EE	Particle Size	Zeta Potential
		mg	mg	mg	%	nm	mV
6	1	90	0	30	54	370.8	-3.3
4	2	90	30	0	80.25	654	-34
2	3	90	0	0	25.2	438.5	-7.5
19	4	80	15	15	64.6	268	-25.3
20	5	80	15	15	64.6	268	-25.3
14	6	80	15	40.2269	61.8	325	-4.1
1	7	70	0	0	15.6	495	-6
8	8	90	30	30	28	145	-24.8

13	9	80	15	-10.2269	46	618	-4.1
15	10	80	15	15	64.6	280	-25.3
7	11	70	30	30	59.5	325	-15.6
17	12	80	15	15	64.6	268	-25.3
16	13	80	15	15	64.6	268	-25.3
18	14	80	15	15	64.6	268	-25.3
11	15	80	-10.2269	15	59.47	450	-3.6
10	16	96.8179	15	15	35.44	366.9	-21.7
9	17	63.1821	15	15	36.85	760	-4
12	18	80	40.2269	15	74.97	269.3	-41.8
5	19	70	0	30	74	650	-2.8
3	20	70	30	0	76.5	724.3	-20.4

Effect of Independent variables (Soya Lecithin, Span 80 and Tween 80) on Entrapment Efficiency (EE %) of Transferosomes [20]

Soya lecithin acts as a lipid component, forming the bilayer structure of transferosomes. Increasing the concentration of soya lecithin typically increases EE% due to enhanced bilayer stability and lipid content. However, excessively high concentrations may cause aggregation, leading to reduced EE%. Span 80 is a non-ionic surfactant that contributes to the vesicle size and stability. An optimal concentration of Span 80 enhances EE% by stabilizing the vesicle structure. Higher levels may reduce EE% due to increased interfacial tension, causing vesicle instability. Tween 80 affects the flexibility and fluidity of the transferosome membrane. A moderate concentration of Tween 80 improves EE% by enhancing the bilayer's fluidity, allowing better encapsulation. Excessive amounts can destabilize the membrane, causing leakage and reduced EE%. At moderate concentrations of Soya Lecithin and Span 80 result in optimal vesicle formation, improving EE%. High levels lead to aggregation or precipitation, reducing EE%. The optimal combination of soya lecithin, Tween 80, and Span 80 maximizes entrapment efficiency. A quadratic regression equation derived from the Box-Behnken model predicts EE% as a function of the three factors. Response surface plots and contour diagrams can be used to visualize the effects and determine the optimal formulation as shown in Figure 9. Fine-tuning these factors ensures optimal drug encapsulation, critical for enhancing the efficacy of transferosomal formulations.

The equation in terms of coded factors can be used to make predictions about the response for given levels of each factor. By default, the high levels of the factors are coded as +1 and the low levels are coded as -1. The coded equation is useful for identifying the relative impact of the factors by comparing the factor coefficients.

$$EE: +64.60-2.97 A +7.43B +3.26C -2.17AB -8.11AC -19.56BC -10.07A^2 +0.9154 B^2 -3.79C^2$$

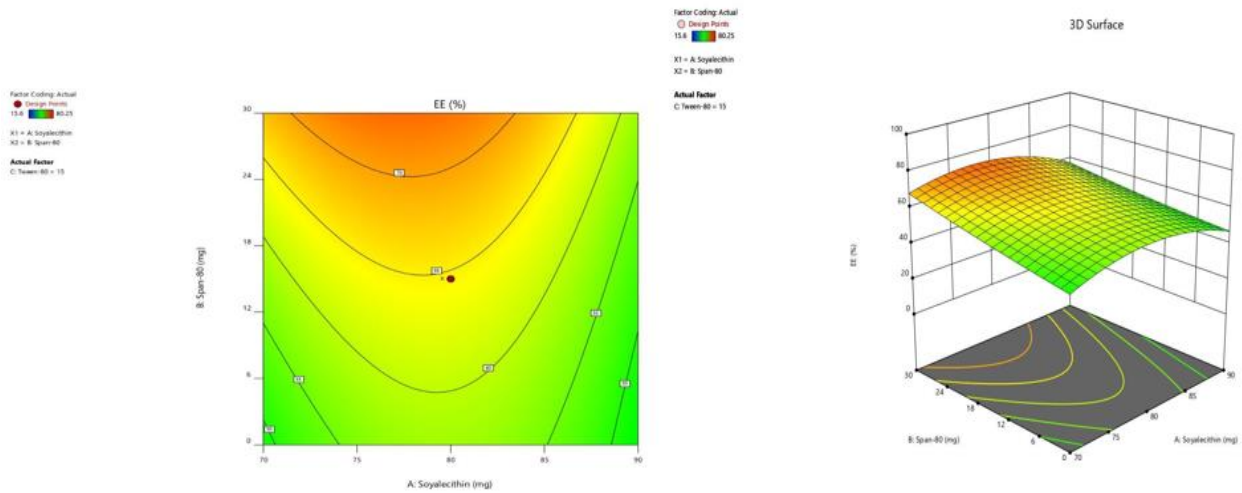


Figure 9: Surface response and counter plot showing the effect of independent variables on Entrapment Efficiency (EE %) of formulated Transfersomes

The two plots represent statistical diagnostic analyses for a model predicting entrapment efficiency (EE). Normal plot of residuals assesses whether the residuals (differences between observed and predicted values) follow a normal distribution. The data points align closely with the red diagonal line, suggesting that the residuals are approximately normally distributed. The residuals are scattered randomly around the horizontal zero line, without a visible trend or pattern. All residuals lie within the red control limits (± 4.41), indicating no significant outliers or influential points. The randomness of the residuals confirms that the model has accounted for systematic effects, and no strong bias exists in the prediction. The diagnostic plots validate the reliability of the model as shown in the figure 10. The normality of residuals and the absence of systematic patterns suggest that the model is robust and provides accurate predictions for entrapment efficiency (EE). These results support the adequacy of the selected model in explaining the relationship between the factors studied (Soya Lecithin, Tween 80, Span 80) and EE.

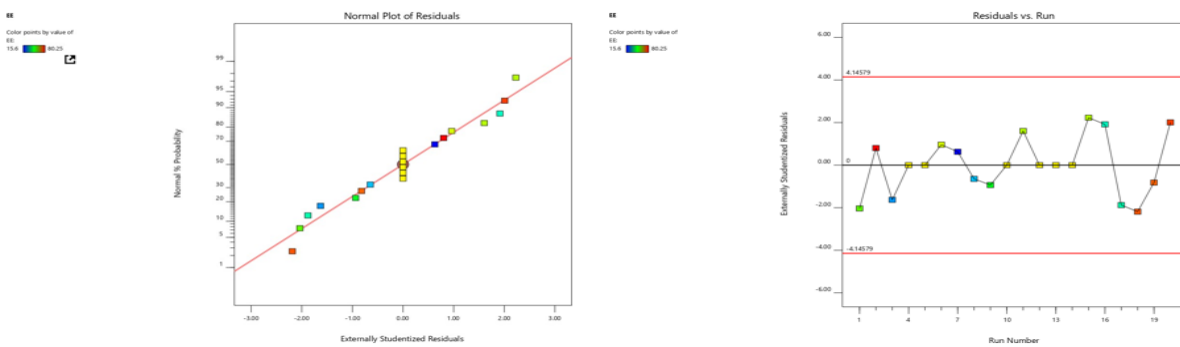


Figure 10: Normal and residual plots showing actual and predicted values for entrapment efficiency

Effect of Independent variables (Soya Lecithin, Span 80 and Tween 80) on Particle size of Transfersomes

Soya lecithin forms the bilayer of transfersomes, contributing to their structural integrity. Increasing soya lecithin concentration leads to larger particle sizes due to the thicker and more stable bilayer formation. Excessive concentrations can cause aggregation, further increasing the particle size. Span 80 affects vesicle stability and surface tension. Low to moderate levels of Span 80 reduce particle size by stabilizing the vesicles. Higher concentrations increase particle size due to changes in interfacial tension, leading to vesicle fusion. Tween 80, a surfactant, influences membrane fluidity and reduces vesicle size by stabilizing lipid dispersions. Moderate concentrations of Tween 80 reduce particle size by enhancing vesicle elasticity and dispersibility. Excessive levels can disrupt vesicle formation, leading to variability in size. At optimal concentrations, these factors minimize particle size by balancing bilayer stability and interfacial tension. High concentrations result in larger particles due to aggregation.

The Box-Behnken design demonstrates that interactions between these factors significantly influence particle size, allowing for precise formulation adjustments to meet desired specifications for pharmaceutical applications. A quadratic regression equation predicts the particle size based on the three factors. Response surface plots and contour diagrams illustrate the interplay

between soya lecithin, Span 80, and Tween 80 showing the regions of optimal particle size. Soya lecithin increases particle size due to bilayer formation, while Tween 80 and Span 80 reduce it by enhancing flexibility and stability. This model helps to identify the region of maximum desirability, balancing the effects of all three factors as shown in figure 11. An optimal formulation minimizes particle size, enhancing the transferosomes efficiency for pharmaceutical applications.

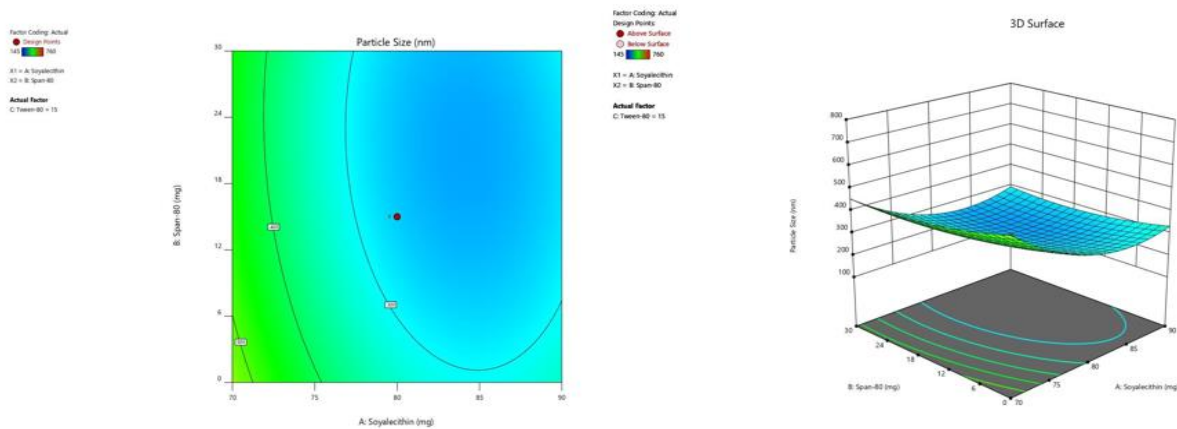


Figure 11: Surface response and counter plot showing the effect of independent variables on particle size of formulated Transferosomes

$$PS: 270.044 + 91.3177A + 30.0142B + 96.1982 C + 10.675 AB - 41.55 AC - 124.45BC + 103.463A^2 - 31.4086 B^2 - 70.9535 C^2$$

The diagnostic plots confirm that the model is statistically valid. The absence of systematic trends and outliers implies that the model effectively explains the influence of Soya Lecithin (mg) on particle size. The normality of residuals (left plot) and the randomness of residuals concerning Soya Lecithin (right plot) as shown in the figure 12 indicate that the model adequately explains the effects of Soya Lecithin on particle size without introducing bias or major errors.

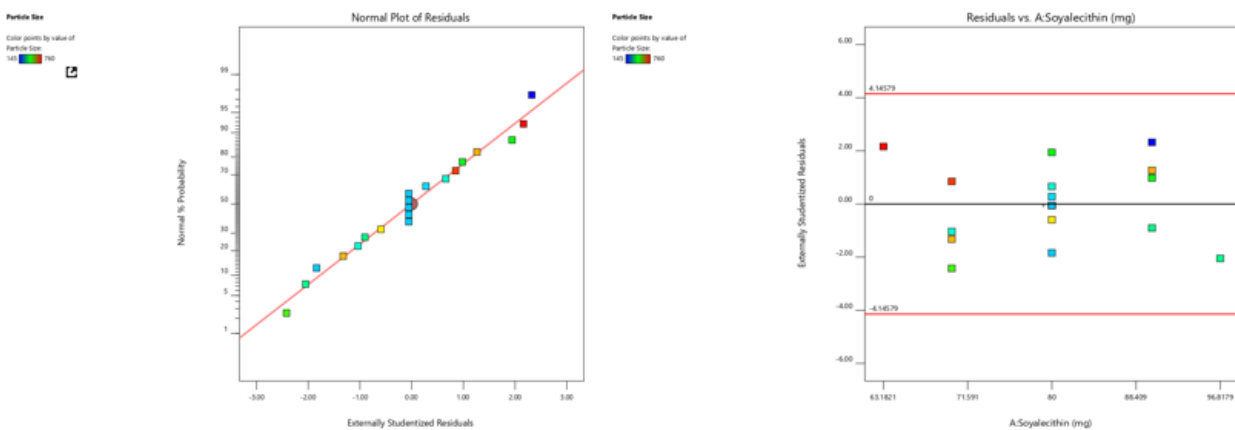


Figure 12: Normal and residual plots showing actual and predicted values for particle size

Effect of Independent variables (Soya Lecithin, Span 80 and Tween 80) on zeta potential of Transferosomes

Zeta potential is a measure of the surface charge of transferosomes, which reflects their stability in dispersion. A higher absolute value of zeta potential (positive or negative) indicates better stability due to electrostatic repulsion between particles, preventing aggregation. Soya lecithin imparts negative charge due to the presence of phosphatidylcholine groups. Increasing the concentration, enhances the negative zeta potential due to a higher density of charged lipid molecules on the vesicle surface, improving stability. But the excessive concentration may saturate the surface, leading to charge neutralization and reduced zeta potential. Span 80 influences vesicle interfacial properties and charge distribution. At low to moderate concentration helps to stabilize the vesicle surface, indirectly supporting higher zeta potential. But at higher concentration, leads to the disruption of

charge uniformity and reducing the zeta potential stability. Tween 80 is a neutral surfactant that affects the bilayer's fluidity but does not directly contribute to charge. At moderate concentration may slightly increase zeta potential by reducing aggregation and improving vesicle dispersion. Excessive concentration can lead to charge shielding due to excessive surfactant adsorption, decreasing zeta potential.

Balanced levels of soya lecithin and span 80 enhance zeta potential by stabilizing vesicle structure and maintaining a consistent charge distribution. Excess Span 80 can reduce surface charge uniformity, lowering zeta potential. The quadratic regression model provides a predictive equation for zeta potential based on the three factors. Response surface plots and contour diagrams illustrate how the combined effects of soya lecithin, Tween 80, and Span 80 impact zeta potential as shown in figure 13. Optimal concentrations of these components result in higher absolute zeta potential values, ensuring better vesicle stability. The optimal formulation ensures a high absolute zeta potential value, ensuring colloidal stability and preventing aggregation, critical for effective drug delivery applications

$$ZP: -25.2414 + 3.99563A + 10.2106 B + 1.56698 C -2.6 AB + 0.675 AC -0.825 BC + 4.01845A^2 -0.535954 B^2 +7.11205 C^2$$

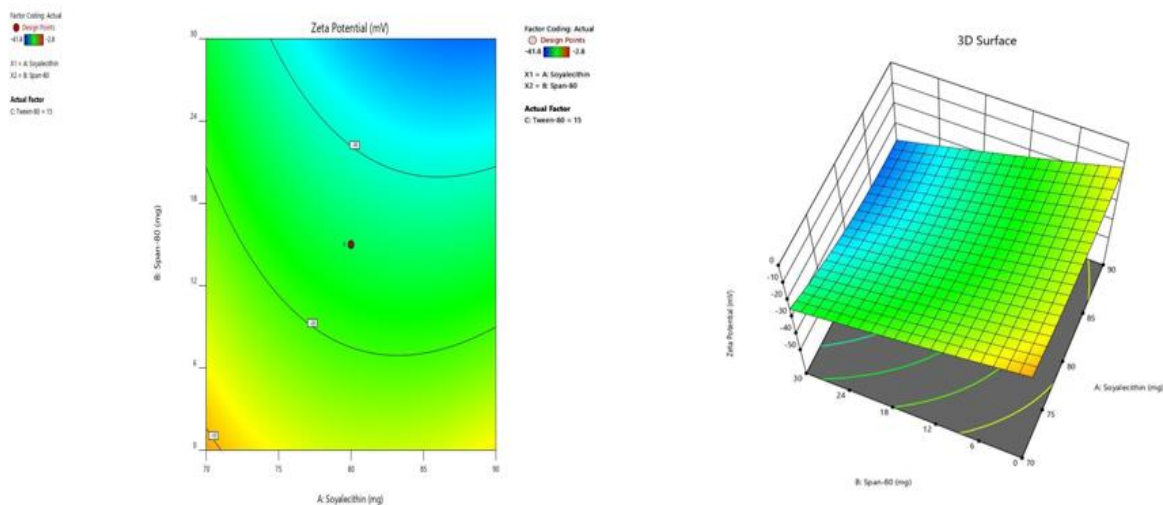


Figure 13: Surface response and counter plot showing the effect of independent variables on zeta potential of formulated Transfersomes

The two plots provide statistical diagnostic information regarding the residuals for the zeta potential of transfersomes. The normality assumption is mostly met, confirming that the model's residuals behave as expected for a reliable statistical model. To check for patterns or systematic trends in the residuals relative to the predicted zeta potential values, which could indicate issues in the model. The residuals are scattered randomly around the horizontal zero line, showing no apparent trend or bias. The diagnostic plots confirm that the model for predicting zeta potential is statistically robust. The residuals are normally distributed (left plot) and show no patterns or trends when compared to the predicted values (right plot) as shown in the figure 14. This suggests that the model provides reliable and unbiased predictions of the zeta potential for transfersomes.

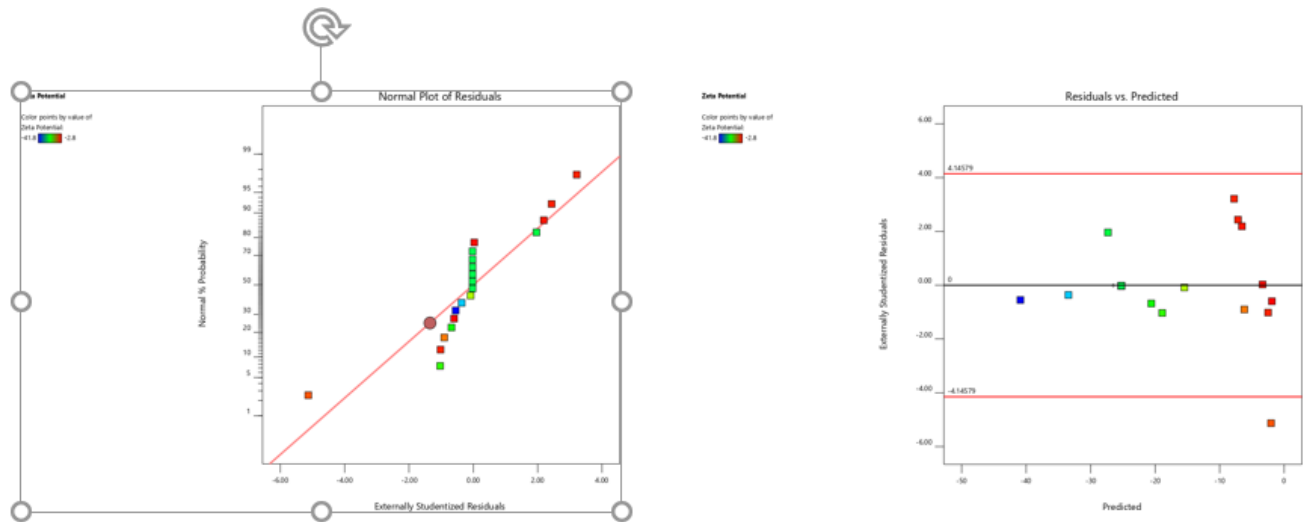


Figure 14: Normal and residual plots showing actual and predicted values for zeta potential

Every response was tuned to a different limit for entrapment efficiency, particle size, and zeta potential in order to create the overlay graph. Every variable that was selected was present in the design space. When the independent variable concentrations were at their optimal levels, the combined desirability plot of all replies showed a maximum D value of 0.884, which was placed on the contour plot of the critical responses.

By applying this desirability method, a formulation consisting of 23.3146 mg of Tween-80, 30 mg of Span-80, and 85.2059 mg of Soya Lecithin could potentially satisfy the criteria for the ideal formulation. An EE of 78.5125 percent, a particle size of 145 nm, and a zeta potential of -33.5546 mV could therefore be obtained by using these ideal concentrations. The formulation and evaluation of an enhanced formulation of transferosomes comprising Miconazole Nitrate and Clotrimazole was done using these predicted optimal concentrations as shown in figure 16. Theoretical values were compared with experimental data in order to confirm the experimental design. The design's accuracy was confirmed by the observation of less than 3 percent relative error.

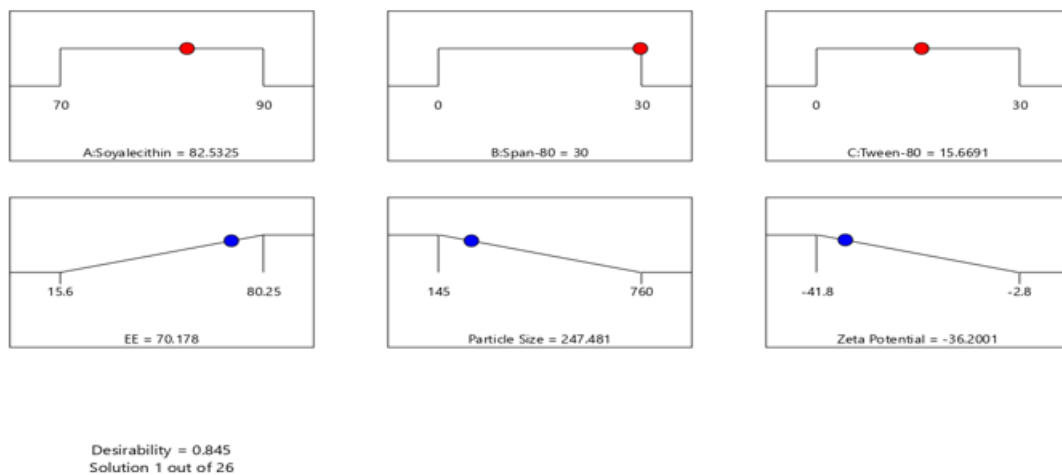


Figure 15: Ramp and Bar Graphs of optimized formula

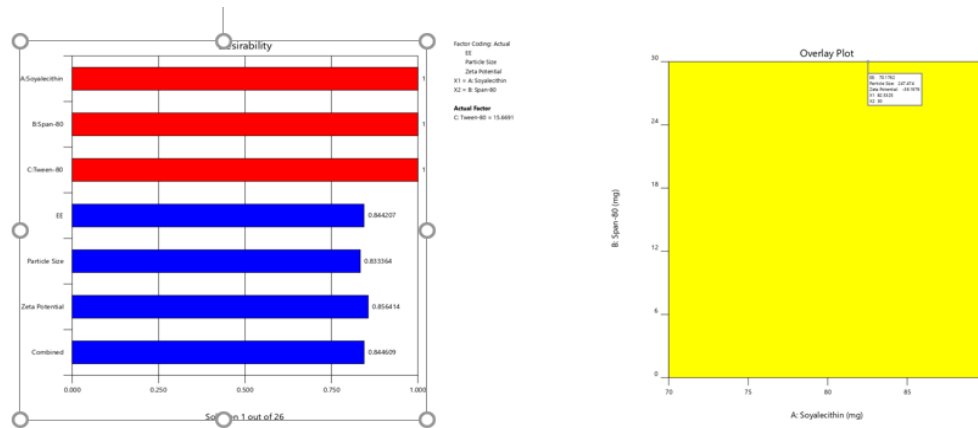


Figure 16: Desirability graphs and overlay plot of optimized formula

Every response was assigned to the quadratic model based on the fit summary and the sequential sum of squares (Type-I). R^2 , p-value, and F-value analyses were done in order to choose a model. Furthermore, the quadratic model has the highest degree of statistical significance in terms of polynomial order, with a p-value of 0.0001. The Desirability Function may be used to find the optimal values for the variables. The viability of utilizing the model to navigate the design space is verified by ensuring adequate accuracy. A ratio greater than 4 is desirable in all dependent variables with adequate precision as shown in table 6. All dependent variables' actual R^2 values were near their predicted values. A more excellent R^2 value, as stated by particle size indicates a more realistic representation of the response by the mean.

Table 6: Model statistical summary. ANOVA Regression analysis of model responses and model fit statistics

Response	Models	R^2	Adju. R^2	Pred. R^2	Adequate Precision	Sequential P-value	Remarks
EE%	Linear	0.1581	0.0003	0.5116		0.4175	
	2F1	0.7197	0.5904	0.3478		0.0020	
	Quadratic	0.9746	0.9518	0.8062	22.927	<0.0001	Suggested
	Cubic	1.0000	0.9997	- 0.4023		<0.0001	Aliased
PS	Linear	0.4094	0.2987	0.0471		0.0340	
	2F1	0.6341	0.4653	0.0734		0.0918	
	Quadratic	0.9769	0.9561	0.8216	22.972	<0.0001	Suggested
	Cubic	0.9998	0.9994	0.9976		<0.0001	Aliased
ZP	Linear	0.6218	0.5509	0.4121		0.0011	
	2F1	0.6453	0.4816	0.2457		0.8344	
	Quadratic	0.9763	0.9550	0.8192	21.821	<0.0001	Suggested
	Cubic	0.9961	0.9876	0.1380		0.0157	Aliased

Characterisation of Transferosomes

Microscopic observation of prepared transferosomes:

The shape of the prepared transferosome formulation was observed using an optical microscope equipped with a camera attachment and found to be spherical with round bilayer structure.

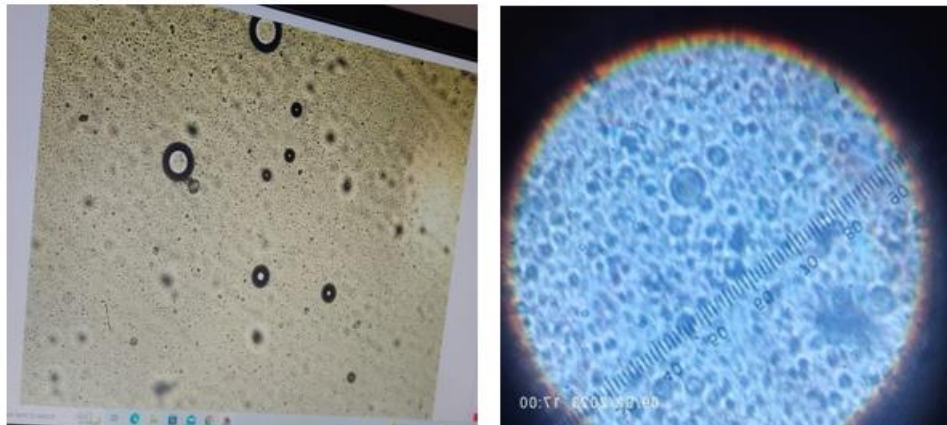


Figure 17: Microscopic observation of prepared Transferosomes

Determination of entrapment efficiency, particle size and zeta potential:

It was found that the prepared MI-CTM transferosomes exhibited a good percentage of entrapment (EE %), with values ranging from (15.6 %) for TFS-7 to (80.25%) for TFS-2. It shows an increase in the concentration of span- 80 shows increase in the entrapment efficiency as compared to the concentration of tween- 80 and also improves the stability of transferosomes. The produced transferosomes underwent particle size analysis, as depicted in figure 18. Between 145 and 724.3 nm is the range of particle size. It was discovered from the particle size results that all of the generated MI-CTM transferosomes have particles smaller than 1000 nm, making them suitable for topical and local applications. The obtained results indicate that, in comparison to tween-80, the particle size of MI-CTM transferosomes generated with Span-80 is larger.

A measurement of the surface potential of suspended particles is called the zeta potential. Because the repelling force of the same charge can prevent particle aggregation, particles with zeta potentials larger than (+) or (-) 20 mV are regarded as stable. The degree of electrostatic repulsion between particles that keeps them from aggregating during storage is represented by the zeta potential, a metric that indicates the stability of TFS dispersion. The stability of TFS dispersion requires a zeta potential of either more than +20 mV or less than -20 mV. The prepared transferosomes shows results ranging from -2.8 to -41.8 mV as shown in figure 19.

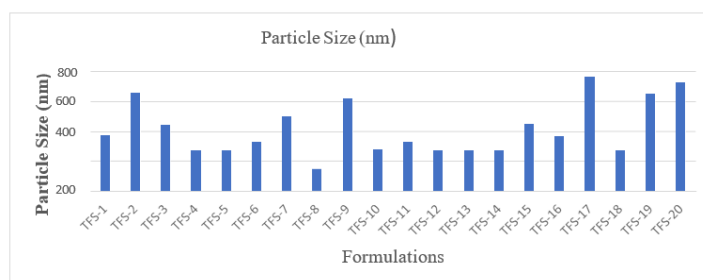


Figure 18: Particle Size of MI-CTM Loaded Transferosomes

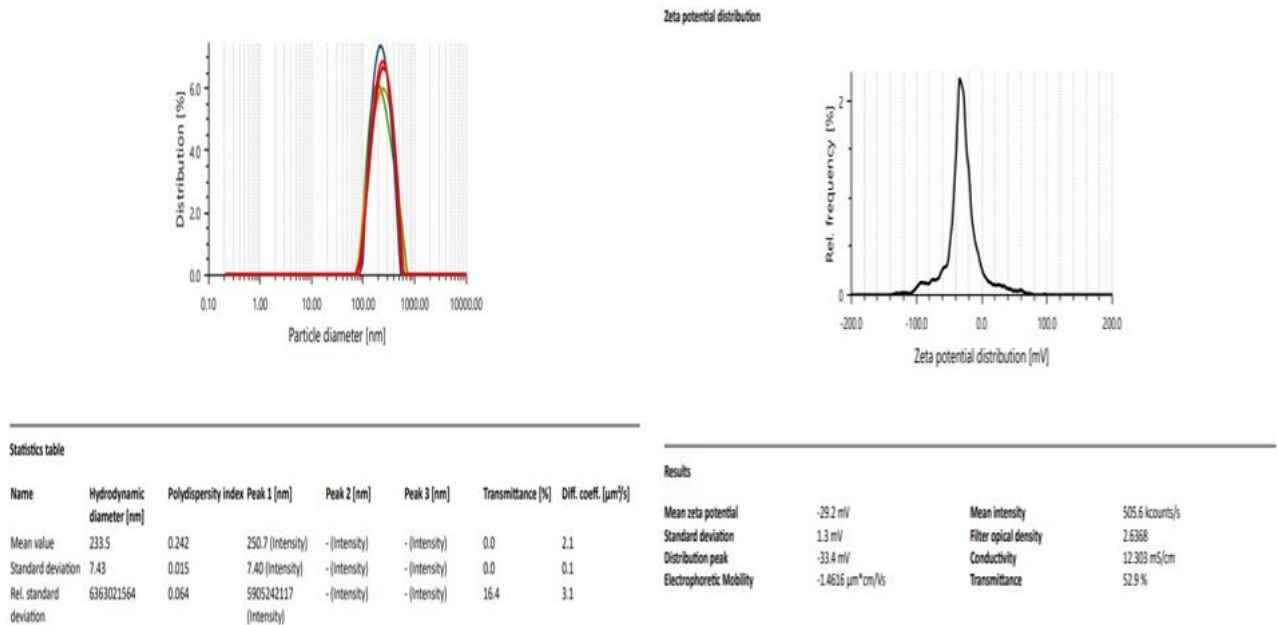


Figure 19: Particle size and Zeta Potential of prepared optimized formulation

SEM (Scanning electron microscopy) Studies

Scanning electron microscopy were used to evaluate the surface morphology of the optimized transfersome. Transfersomes typically appear as spherical or slightly oval-shaped vesicles under SEM. The surface of the vesicles was smooth and uniform, indicating successful formation and encapsulation. Few sporadic vesicles with a homogeneous size distribution and retained their structural integrity with minimum aggregation, indicating good colloidal stability of formulation as shown in figure 20. The uniform dispersion and intact vesicle structure indicate the suitability of the transfersomes for drug delivery applications

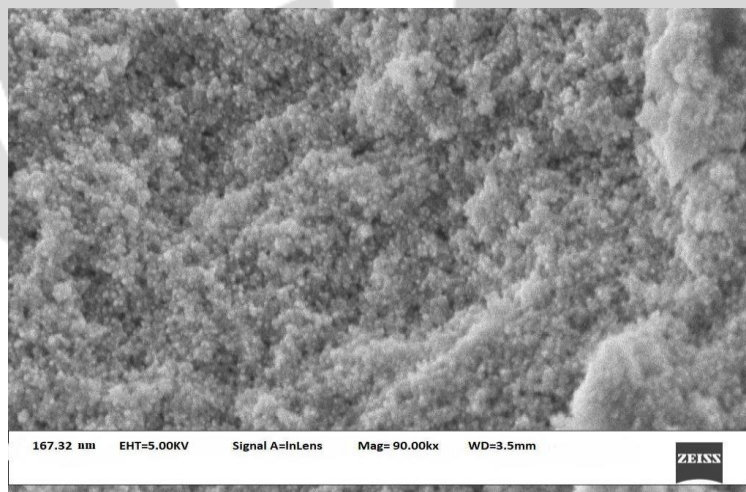


Figure 20: SEM of Optimized Transfersosomal Gel

Evaluation of Optimized MI-CTM loaded Transfersosomal Gel

Homogeneity

To verify that there is no phase separation, syneresis (water evaporating from a gel), or foreign matter present, a visual homogeneity test for the therapeutic product may be helpful, at least for an initial batch. The transfersosomal gel that was loaded with MI-CTM had an optimised formulation that was uniformly smooth.

pH determination

A calibrated pH meter was used to measure the pH of topical gels. Three average samples were used to obtain the readings. The pH of optimised formulation was found to be 6.99 ± 0.40 , which is compatible with human skin and making the gel suitable for topical or transdermal applications without causing irritation as it is close to neutral pH 7. A stable pH within this range ensures the stability of the transferosomes, as extreme pH variations can degrade vesicle integrity or the active pharmaceutical ingredient.

Spreadability

The spreadability rating shows how easily the gel can be spread with a little shear force. The topical gel based on carbopol was shown to have a spreadability within the range of $5.43-7.30 \pm 0.460$ g.cm/sec, meaning that it may be easily spread on skin surfaces with minimal stress.

Drug content estimation

Using a UV Spectrophotometer, the drug content was estimated. Drug content of the optimized formulation was found to be 96.45% and 94.85% w/w for miconazole nitrate and clotrimazole respectively which represents good content uniformity.

Viscosity and Rheological studies

Using spindle no. 4, the viscosity and rheological characteristics of the MI-CTM loaded topical gel were measured using a Brookfield digital viscometer. The ratio of solid to liquid fraction, which creates the structure, determines the consistency of a gel system. Around 16640 cps at 5 rpm was discovered to be the range of viscosity for the topical gel loaded with MI-CTM. A shear rate v/s viscosity graph, as shown in figure 21, was used to analyse the rheological properties of the formulations.

This demonstrated how the formulations viscosity lowers when the shearing rate rises, indicating pseudoplastic flow characteristics and non-Newtonian flow (shear thinning). The colloidal network structure that aligns itself in the direction of shear causes this pseudoplasticity, which causes the viscosity to decrease as the shear rate rises.

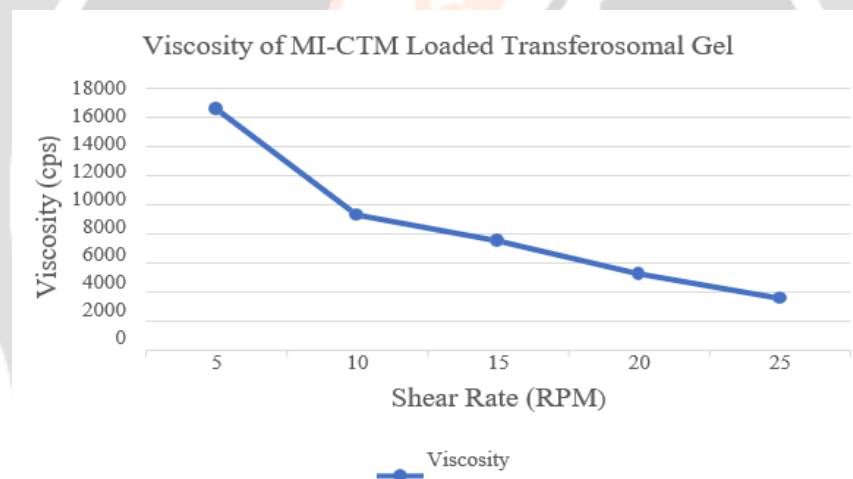


Figure 21: Rheological Profile of MI-CTM Loaded Transferosomal Gel

In vitro drug release studies

To estimate how consistently the rate and duration of medication release will occur, drug release studies are necessary. For the MI-CTM topical gel drug release performance to be guaranteed, it has long been known that polymer dissolution plays a crucial role in drug release from matrices. Underwent an in-vitro drug release study for 30 min to 24 h in order to examine the drug releases from the MI-CTM loaded transferosomal gel bearing topical gel. Figure 22 displays the MI-CTM loaded transferosomal gel containing topical gel's *in vitro* release profiles. For optimised formulation, the *in vitro* drug release data was determined to be in the highest order. In a 24 h period, the total percentage of drug release was recorded. For miconazole nitrate and clotrimazole, the drug release of MI-CTM loaded transferosomes bearing topical gel was reported to be 86.94% and 89.87% in 24 h, respectively.

The *in vitro* drug release from MI-CTM loaded transferosomal gel was fit into an appropriate mathematical model in order to be predict and correlate the release patterns. Several kinetic equations (Zero order, first order, Higuchi's equation, Hixon Crowell, and Korsmeyer-Peppas) were used to investigate the drug release from the transferosomal gel. Upon comparing the respective correlation coefficients, it was discovered that the drug miconazole nitrate followed first order kinetics dominantly, with a correlation coefficient closer to 1 (0.9973) than zero order (0.9097), Peppas model (0.9915), and Higuchi model (0.99), and for the drug clotrimazole, it followed Peppas model dominantly, with a correlation coefficient closer to 1 (0.9925) than zero order (0.9221), First order (0.9595), and Higuchi model (0.9892). Additionally, the data were fitted into Korsmeyer Peppas' exponential model, $M_t / M_a = K_{tn}$, in order to comprehend the drug release mechanism. The drug transport mechanism is characterised by the values of 'n' for the release exponent, 'k' for the kinetic constant, and 't' for the fraction of drug released after

time 't'. The values for "n" fell between 0.45 to 0.89, indicating that the non-Fickian transport mechanism for both drugs was used for the *in vitro* drug release from these transferosomal gels.

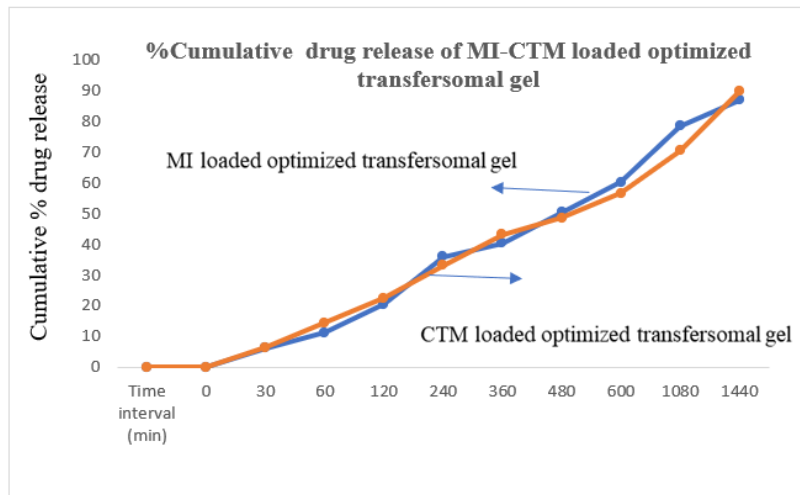


Figure 22: *In vitro* drug release profile of optimized formulation

Stability studies

The stability studies were carried out at 4°C ±2°C and 25°C±2°C/60% RH, for a period of 3 months. MI-CTM loaded transferosomal gels was analysed for pH, drug content and *in-vitro* release studies. Results from the stability studies showed that there was no significant change in the pH, drug content and *in-vitro* release behaviors of the transferosomal gels as shown in table 7. Hence prepared transferosomal gels formulation was physicochemical stable throughout study period.

Table 7: Stability Studies for Optimized Transferosomal Gel

Months	4°C±2°C					25°C/60% RH				
	pH	Drug content (%)		% CDR		pH	Drug content (%)		% CDR	
		MI	CTM	MI	CTM		MI	CTM	MI	CTM
Initial	6.99±0.4	96.45±0.5	94.85±0.2	86.9±0.1	89.8±0.1	6.99±0.4	96.45±0.5	94.85±0.2	86.9±0.2	89.9±0.1
1	6.96±0.2	96.43±0.5	94.83±0.6	86.6±0.1	89.8±0.1	6.96±0.2	96.43±0.5	94.83±0.6	86.1±0.1	89.6±0.2
2	6.95±0.4	96.30±0.6	94.85±0.5	86.5±0.1	89.8±0.1	6.95±0.4	96.30±0.6	94.85±0.5	86.1±0.3	89.3±0.3
3	6.92±0.2	96.28±0.3	94.82±0.4	86.2±0.1	89.8±0.1	6.92±0.2	96.28±0.3	94.82±0.4	86.2±0.2	89.1±0.2

CONCLUSION

The prepared antifungal transferosome gels hold significant promise for advancing topical antifungal therapies. Their ability to enhance drug penetration through the skin and ensure targeted delivery to infected areas makes them highly effective against stubborn fungal infections like cutaneous candidiasis, athlete’s foot, and ringworm. By incorporating active pharmaceutical ingredients like clotrimazole or miconazole, transferosome gels can improve bioavailability, reduce dosing frequency, and

minimize side effects compared to conventional formulations. The Miconazole nitrate and clotrimazole loaded transferosomes were prepared by thin film hydration method, which sustained the drug release for prolonged period of time and might be useful in treatment of fungal infection and optimized by Box-Behnken Design utilizing different amounts of soy lecithin, span 80, and tween 80. The particle size of optimized transferosomal gel was found in the range of 233.5 nm, hence effective for transdermal applications. For the preparation of transferosomal gel, carbopol 940P is used as the gel base and the gel was subjected to determine different properties of gels such as pH, spreadability, viscosity, drug content, and *in-vitro* diffusion studies. All the results were found to be satisfactory.

Recent patents focus on enhancing stability, using natural edge activators, targeted delivery, nano-transferosomes, and photoprotective gels. These innovations demonstrate the potential of transferosome gels to revolutionize pharmacy by offering safe, efficient, and patient-friendly drug delivery systems across therapeutic, cosmetic, and diagnostic domains. In the future, these gels could be further developed for systemic fungal infections by exploring their transdermal delivery capabilities. With ongoing research, these gels could incorporate natural antifungal compounds or nano-drug carriers for enhanced efficiency and safety. Overall, antifungal transferosome gels represent a promising frontier in dermatological and pharmaceutical applications, meeting the demand for effective, patient-friendly, and advanced fungal infection treatments.

REFERENCES

1. Patel V, Sharma OP, Mehta T. Nanocrystal: A novel approach to overcome skin barriers for improved topical drug delivery. Expert opinion on drug delivery. 2018 Apr 3;15(4):351-68.
2. Bagde SA, Jadhav N, Mali N, Karpe M. Comparison of *in vitro* Antifungal Studies of Different Bifonazole Formulations with Marketed Bifonazole Formulation. International Journal of Pharmaceutical Chemistry and Analysis. 2016 Feb 15;2(4):187-91.
3. Shilakari G, Singh D, Asthana A. Novel vesicular carriers for topical drug delivery and their application's. International Journal of Pharmaceutical Sciences Review and Research. 2013;21(1):77-86.
4. Patil PB, Datir SK, Saudagar RB. A Review on Topical Gels as Drug Delivery System. Journal of Drug Delivery and Therapeutics. 2019 Jun 15;9(3-s):989-94.
5. Rai S, Pandey V, Rai G. Transferosomes as versatile and flexible nano-vesicular carriers in skin cancer therapy: The state of the art. Nano reviews & experiments. 2017 Jan 1;8(1):1325708.
6. Jadupati M, Amites G, Kumar NA. Transferosomes: an opportunistic carrier for Transdermal drug delivery system. International Journal of Pharmacy IRJP. 2012;3(3):35-8.
7. Chauhan N, Kumar K, Pant NC. An updated review on transferosomes: a novel vesicular system for transdermal drug delivery. Universal Journal of Pharmaceutical Research. 2017;2(4):49-52.
8. Abdellatif MM, Khalil IA, Khalil MA. Sertaconazole nitrate loaded nano vesicular systems for targeting skin fungal infection: *in-vitro*, *ex-vivo* and *in-vivo* evaluation. International journal of pharmaceutics. 2017 Jul 15;527(1-2):1-1.
9. Joshi A, Kaur J, Kulkarni R, Chaudhari R. *In-vitro* and *ex-vivo* evaluation of raloxifene hydrochloride delivery using nano-transferosome based formulations. Journal of Drug Delivery Science and Technology. 2018 Jun 1;45:151-8.
10. Ghanbarzadeh S, Arami S. Formulation and evaluation of piroxicam transferosomal gel: An approach for penetration enhancement. Journal of drug delivery science and technology. 2013 Jan 1;23(6):587-90.
11. Himabindu Peddapalli & G.V Radha. Formulation and optimization of novel vesicular elastic carrier for transdermal delivery of lercanidipine for the treatment of hypertension Materials Today: Proceeding 2023.
12. Ramkanth S, Anitha P, Gayathri R, Mohan S, Babu D. Formulation and design optimization of nano-transferosomes using pioglitazone and eprosartan mesylate for concomitant therapy against diabetes and hypertension. European Journal of Pharmaceutical Sciences. 2021 Jul 1;162:1-11.
13. Yusuf M, Sharma V, Pathak K. Nanovesicles for transdermal delivery of felodipine: development, characterization, and pharmacokinetics. International journal of pharmaceutical investigation. 2014 Jul;4(3):119-130.
14. Chaudhary H, Kohli K, Amin S, Rathee P, Kumar V. Optimization and formulation design of gels of Diclofenac and Curcumin for transdermal drug delivery by Box- Behnken statistical design. Journal of pharmaceutical sciences. 2011 Feb 1;100(2):580-93.
15. Antimisariaris SG, Marazioti A, Kannavou M, Natsaridis E, Gkartziou F, Kogkos G, Mourtas S. Overcoming barriers by local drug delivery with liposomes. Advanced drug delivery reviews. 2021 Jul 1;174:53-86.
16. Alkhalidi HM, Hosny KM, Rizg WY. Oral gel loaded by fluconazole–sesame oil nano-transferosomes: development, optimization, and assessment of antifungal activity. Pharmaceutics. 2020 Dec 25;13(1):27.
17. Patel P, Patel P, Mahajan A, Koradia S, Saluja A, Shah K. Formulation, Evaluation, and Optimization of Diacerein Loaded Transferosomal Gel for Arthritis. Optimization. 2022 Apr 28;13(2):7-16.
18. Chandana Setty Sharaff, Pranay Renukuntla, Himabindu Peddapalli, Mounika Kuchukuntla, Vasudha Bakshi, Rajendra Kumar Jadi. Formulation, Development, and Characterization of Loratadine Emulgel. Journal of Applied Pharmaceutical Research, 2024, 12 (2): 52 – 60.

19. Das B, Sen SO, Maji R, Nayak AK, Sen KK. Transfersomal gel for transdermal delivery of risperidone: Formulation optimization and ex vivo permeation. *Journal of Drug Delivery Science and Technology*. 2017 Apr 1;38:1-23.
20. Himabindu Peddapalli, G.V. Radha, Santhosh Kumar Chinnaiyan. Formulation optimization and PK/PD evaluation of novel valsartan bilosomes enhancing transdermal drug delivery. *Journal of Drug Delivery Science and Technology*, 92 (105400), 1-16 (2024).
21. Verma N, Jain S, Gupta N, Kapoor V, Rajput D. Formulation, Development and Evaluation of Transfersomal Gel of Amphotericin B. *Journal of Advanced Scientific Research*. 2019 Dec 10;10(04 Suppl 2):254-60.
22. Tamilarasan N, Yasmin BM, Anitha P, Umme H, Cheng WH, Mohan S, Ramkanth S, Janakiraman AK. Box–Behnken design: optimization of Proanthocyanidin-loaded Transfersomes as an effective therapeutic approach for osteoarthritis. *Nanomaterials*. 2022 Aug 26;12(17):2954.
23. Kharwade R, Ali N, Gangane P, Pawar K, More S, Iqbal M, Bhat AR, AlAsmari AF, Kaleem M. DOE-Assisted Formulation, Optimization, and Characterization of Tioconazole-Loaded Transfersomal Hydrogel for the Effective Treatment of Atopic Dermatitis: In Vitro and In Vivo Evaluation. *Gels*. 2023 Apr 4;9(4):303.
24. Gayathri H, Sangeetha S. Design and development of tofacitinib citrate loaded transfersomal gel for skin cancer by box-Behnken design-doe approach. *Int. J. Health Sci*. 2022; 6:3119-40.
25. Patel P, Patel P, Mahajan A, Koradia S, Saluja A, Shah K. Formulation, Evaluation, And Optimization of Diacerein Loaded Transfersomal Gel for Arthritis. *Pharmacophore an International Journal*. 2022 Apr 28;13(2):7-16.
26. Himabindu Peddapalli, Rajendra Prasad Ganta, Narender Boggula. Formulation and Evaluation of Transdermal Patches for Antianxiety Drug. *Asian Journal of Pharmaceutics*. 2018; 12(2):127-136.

